List, the Structure, and Chemistry of Neutrinium Elements of Light Matter

D. Skripachov

Abstract

Light Matter (LM) is a substance composed of light nuclei of neutrinium (NN) with a mass of 1 to several tens of MeV. It is assumed that neutrinos are able to form short-lived Cooper pairs, some of which quickly decays, and the other part is undergoing fusion, becoming a non-relativistic nuclei of LM. Studying the structure of NN shows that neutrinos can be joined together by 2 types of bonds, alpha and kappa. Chemistry of neutrinium elements (CNE) is studying reactions involving NN, including the synthesis of NE with larger mass number, condensation of NN in molecular aggregations, and annihilation of neutrinium and antineutrinium. CNE allows explain a number of astrophysical phenomena, including sunspots, solar flares and coronal mass ejections, coronal holes, aurora and polar radio emission, Herbig-Haro objects, the radio emission of pulsars, the spiral arms of galaxies and relativistic jets, the emission of quasars, and extragalactic background light.

1. Introduction

Have you ever dreamed to visit the Brazilian carnival? It is so exciting, feel the participant of grand parade! And now imagine for a moment that dark matter performs for us the same sparkling and colorful show! It is impossible, you think, because DM is not for nothing called "dark" and it is absolutely true, that DM does not emit light. But what do we know about DM? Today experiments to search for DM can be divided on two classes, one of which is based on astronomical observations, which revealed the influence of the hidden mass on the rotation of galaxies and bending of light, and the other directed to the registration of radiation in the scintillators and semiconductor detectors from possible collisions of DM particles with the nuclei of atoms. Astronomical observations suggest that the total mass of DM in the universe is about 5.7 times the mass of the baryonic matter. In the second case the experiments do not allow anything to clarify about the properties of DM, except that the latter has a very low propensity to react with ordinary matter. Meanwhile, recent studies have shown that the X-ray spectra of large galaxies contain unexplained excess energy in the 3.5 keV, which fails to match any of the known spectral lines of chemical elements [13], [14]. If this new spectral line really belongs to DM, the latter can no longer be regarded as a "dark", not emitting substance, manifesting itself only by gravitation. But then this means that DM particles should possess all the same properties as the majority of the known elementary particles. On the other hand, the accumulated data on elementary particles are so extensive and systematized, that it seems incredible that DM particles (substance overflowing universe!) somehow did not show yourself in one or another experiment. Or may be manifestations of DM are so ordinary that we simply do not suspect that they surround us? In any case, we must state that the phenomenology of hypothetical DM particles suffers from a lack of interpretation. But now we are going to fill this gap. Our new approach is that scientific model at any level of detail would have had 2 or 3 of different, relevant and complementary interpretation. Adhering to this approach, we will consider a new model of light matter (LM) whose particles are nuclei of neutrinium and antineutrinium consisting of neutrinos and antineutrinos, respectively [2].

According to the neutrino model of LM, at rapprochement of neutrinos by a distance of about 10^{-9} cm arises a Cooper neutrino pair (CNP), which immediately decays or is undergoing a quantum transition, becoming a nucleus of deutrinium. A necessary condition for the emergence of CNP will be crossing neutrino trajectories, which creates the orbital angular momentum opposite to neutrino helicity, otherwise CNP does not arise. Fusion of neutrino pairs (npf-process) will be possible, if the sum of the neutrino energy is not less than the rest mass of deutrinium, that is not less than 1 MeV. Additional condition for fusion will be a requirement of the relative proximity of neutrino energies. Each fusion of CNP must be accompanied by the emission of a photon in the energy range from microwaves to soft X-rays:

$$\nu\nu \rightarrow {}^{2}Nu + \gamma \qquad (1)$$

Depending on the energy of primary neutrinos nuclei of deutrinium will be non-relativistic and ultra-relativistic, and the direction of their movement will repeat the direction of the original neutrinos. Deutrinium nuclei in collisions with each other will form the nucleus of tetrinium. Neutrinium nuclei (NN) with a larger mass number can be synthesized as by joining nuclei of deutrinium, and by combining the more massive nuclei. NN always consist of an even number of neutrinos. Synthesis of tetrinium and more massive neutrinium elements (NE) must be accompanied by the emission of X-ray photons with energies in the range of 2-6 keV:

$${}^{2}Nu + {}^{2}Nu \rightarrow {}^{4}Nu + \gamma \qquad (2)$$

$${}^{4}Nu + {}^{2}Nu \rightarrow {}^{6}Nu + \gamma \qquad (3)$$

Spin and charge of NN are considered to be zero, but the magnetic moment should be nonzero.

2. List and structure of NE

Unlike chemical elements, NE do not have properties of periodicity. Starting with tetrinium they have a nuclear isomers.

Table 1: Neutrinium elements of light matter.

Number of neutrinos	**Number of isomers**	**Designation of elements**	**Name of the element**	**Mass of the nucleus**
2	1	^{2}Nu, Du	deutrinium	~1 MeV
4	6	^{4}Nu, Tt	tetrinium	~2 MeV
6	?	^{6}Nu	hexatrinium	~3 MeV
8	?	^{8}Nu	octatrinium	~4 MeV
...				
20	?	^{20}Nu	icosatrinium	~10 MeV
...				
30	?	^{30}Nu	triacontrinium	~15 MeV
...				

Isomerism of NN deduced from the alleged cubic form of neutrinos and the principle of connection by edges of cubes. It also adopted as a postulate that none of the two unit cells of space related to this connection of two neutrinos by edges of cubes, does not participate in other connections of his own two neutrinos with any other neutrinos. In any connection by edges of cubes both neutrinos are completely equal, so this connection can be considered as a covalent bond. We denote such a connection as alpha bond. For neutrinos connected with alpha bond is applicable the concept of valence and covalence. Neutrino valence (number of actually available alpha bonds) may be 1, 2 or 3, and covalence (the maximum possible number of alpha bonds at a given position) 2 or 3.

Consider the structure of tetrinium isomers. Boundary neutrinos always have covalency 2 or 3. In the linear isomer (Fig. 1, b) two internal neutrinos have a valence of 2 and covalence 2, i.e. fully saturated and are not capable of forming new alfa bonds. In the partially linear (partially branched) iso-para-tetrinium (Fig. 1, c) one internal neutrino has covalency 2 and the other covalency 3. In four fully branched isomers both internal neutrinos have covalency 3. Cis-ortho-tetrinium (Fig. 1, a) can be regarded as a incomplete six-membered ring. Isomers in the positions c, d, e, f are enantiomers.

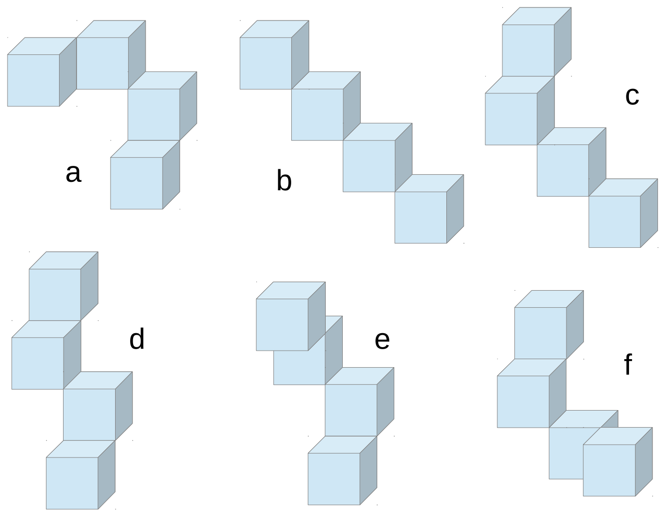

Fig. 1. Structure of nuclear isomers of tetrinium. Names of isomers: a: cis-ortho-tetrinium, b: p-n-tetrinium, c: para-iso-tetrinium, d: trans-meta-tetrinium, e: cis-meta-tetrinium, f: trans-ortho- tetrinium.

Obviously, increasing the mass number, the number of isomers is growing exponentially. But we assume that in reality there is a tendency to spontaneous reduction variety of isomers and the predominance among them nuclei of para- and ortho-neutrinium having respectively linear and polycyclic structure (Fig. 2). We will call the linear nuclei as garlands and polycyclic nuclei as lace. In comparison with other isomers laces and garlands have the least complex relief that gives them the possibility of closer mutual placement, the limit of which will be the connection of NN by vertices of cubes.

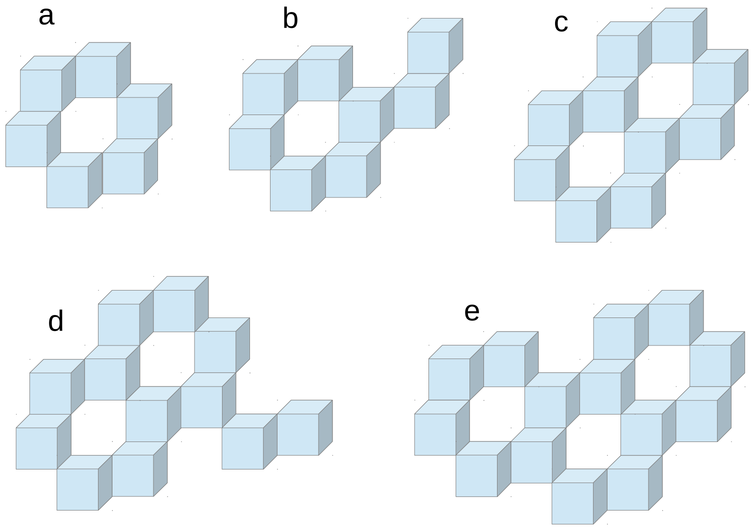

Fig. 2. Structure of the cyclic nuclei ^{6}Nu,^{8}Nu,^{10}Nu,^{12}Nu,^{14}Nu of ortho-neutrinium. a: cyclo-hexatrinium, b: cyclo-octatrinium, c: cyclo-dekatrinium, d: cyclo-dodekatrinium, e: cyclo-tetradekatrinium.

Denote the connection by vertices of cubes as kappa bond. Supposedly kappa bond must be several orders of magnitude weaker than alpha bond. Connecting by the vertices of cubes NN form aggregations in the form of stacks (of laces), asterisks (of garlands), and mixed forms (Fig. 3).

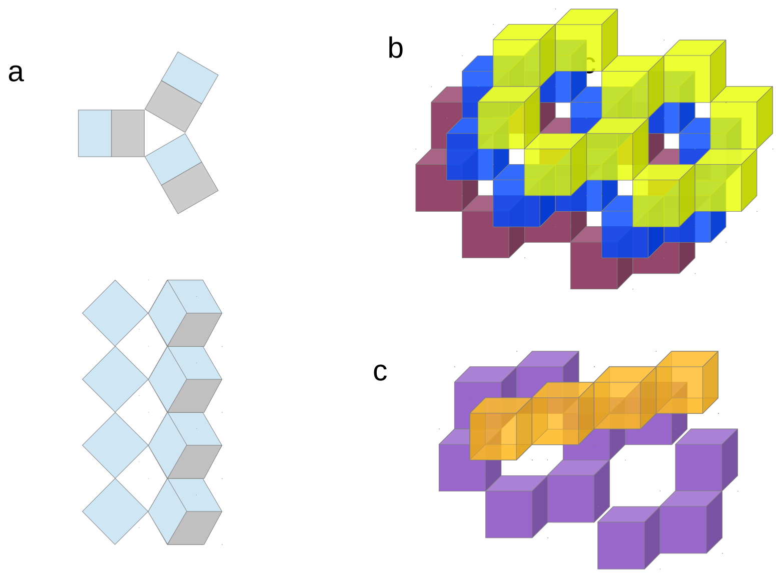

Fig. 3. Aggregations of neutrinium nuclei. a: triple para-tetrinium p-$^{6}Nu_3$, b: triple cyclo-dekatrinium o-$^{10}Nu_3$, c: mixed compound of cyclo-dekatrinium and para-tetrinium o-$^{10}Nu_1$ p-$^{4}Nu_1$.

Structure of NE determines their characteristics and types of reactions in which there is a change of mass number or aggregate state of NN. Chemistry of neutrinium elements (CNE) is studying these reactions.

3. Subject of CNE

Speaking of CNE, we will keep in mind the following reactions:

1) formation and decay of the CNP ($\nu\nu$, $\overline{\nu\nu}$,$\nu\overline{\nu}$), as well as mixed neutrino-lepton pairs (eν, e$\overline{\nu}$, $\overline{e}\nu$, $\overline{e\nu}$);
2) npf-process and synthesis of deutrinium;
3) synthesis of tetrinium and more massive nuclei, as well as their splitting;
4) condensation and decomposition of NN aggregations;
5) annihilation of NE (usually always partial).

Formation and decay of pure neutrino and neutrino-lepton pairs is accompanied by a greater or lesser degree of alignment of the energy and momentum of the particles. Supposedly these reactions are not accompanied by radiation. In cases where close to CNP is the nucleus of deutrinium, fusion probability increases due to induction of npf-process. If in npf-process enters a pair $\nu\overline{\nu}$, then there is annihilation:

$$\nu\bar{\nu} \rightarrow 2\gamma \qquad (4)$$

Synthesis of NE is accompanied by an increase of NE mass numbers up to about 100, and then begins to equilibrate by crushing from collisions with other NN or atomic nuclei and elementary particles. Supposedly NE mass numbers of galactic LM are within the range from 10 to 100, while of LM of stellar origin do not exceed 10.

Condensation of NN leading to the formation of molecular aggregations must be accompanied by radio emission, supposedly at the frequency of 100-150 kHz.

Annihilation of neutrinium and antineutrinium almost always be partial, for example:

$$^{14}\overline{Nu} + {}^{2}Nu \rightarrow {}^{12}\overline{Nu} + \nu + \bar{\nu} + 2\gamma\ , \qquad (5)$$

$$^{10}Nu + {}^{10}\overline{Nu} \rightarrow {}^{8}Nu + {}^{8}\overline{Nu} + \nu + \bar{\nu} + 2\gamma\ , \qquad (6)$$

$$^{6}Nu + {}^{10}\overline{Nu} \rightarrow {}^{4}Nu + {}^{8}\overline{Nu} + e^{-} + e^{+} + 2\gamma \qquad (7)$$

Annihilation energy is distributed in an arbitrary manner between the reaction products. Photons emitted in the annihilation of LM will have a continuous spectrum in a wide range, from infrared to gamma radiation.

4. CNE and solar phenomena

Supposedly solar corona exists due to the energy of neutrino pairs fusion and subsequent synthesis of NE with larger mass number. Apparently, solar neutrinos from ^{7}Be (0.862 MeV), ^{13}N (0÷1.2 MeV), ^{15}O (0÷1.73 MeV), and pep reaction (1.44 MeV) are playing a leading role here. And what about the pp neutrinos? As is known, pp neutrino have energy not higher than 0.42 MeV, that is as if insufficient for fusion of neutrino pairs. However, pp neutrinos and plasma electrons actively react due to proximity of their energy, and form neutrino-electron pairs (NEP), in the decay of which particles exchange with each other a certain amount of energy. Passing NEP chains the most energetic pp neutrinos receive the missing energy and become able to enter into npf-process. In turn, nuclei of deutrinium that are synthesized during npf-process immediately enter the synthesis of more massive NE. Variability of reactions involving pp neutrinos determines the variable nature of such phenomena as sunspots, solar flares and coronal mass ejections. In the depths of a sunspot electrons involved in NEP move to the surface of the sun at an angle, so that their trajectories form a bundle twisted in one or another direction. Depending on the direction of twist, the magnetic field of a sunspot will have a certain polarity. Low temperature of the spot is due to energy transfer from the electrons to the neutrino in the process of formation and decay of NEP. Received the missing energy, neutrinos form Cooper pairs, some of which immediately fused into the nuclei of deutrinium, from which in turn are synthesized nuclei of tetrinium and more massive NE. Each burst of NE synthesis in the photosphere of the sun is accompanied by an X-ray flare. If the outbreak of NEP begins in the deeper layers of the sun, then NE output will be more large-scale. Natural to assume that such a powerful bursts of NE synthesis will be accompanied by a coronal mass ejection. But let us return to the permanent components of the solar corona and pay attention to such a phenomenon as coronal holes (CH). Since the CH are usually located in the polar regions of the sun, it can be assumed that the existence of CH due to the influence of the magnetic field of the sun on the synthesis of NE. In the area of the poles the magnetic field effect is maximized, and the magnetic axis of NN are oriented along the magnetic field lines. Supposedly unidirectional magnetic orientation of NN is not conducive to the synthesis of NE, which is accompanied by the appearance of CH. It should be noted that in the solar corona also occur the condensation of NN into molecular neutrinium (MN), which make some contribution to the radio emission from the sun. A relatively small part of the solar neutrinium is spent on annihilation with the galactic antineutrinium. In general all synthesized neutrinium leaves the sun as part of the solar wind.

5. Auroras and polar radio emission

In a magnetic field of the Earth magnetic axis of NN turn at the intersection of magnetic field lines, and MN partially decomposed to the original NN. This creates a sufficient concentration of NN pairs, whose mutual orientation of the magnetic axes for some time is favorable for the synthesis of NE. X-rays of NE synthesis excites the atoms and molecules of atmospheric gases, mainly in the thermosphere. Such a more or less a permanent effect on the thermosphere is created by NE originating from neutrinos of ^{7}Be, CNO-I cycle, and pep reaction. If we deal with NE originating from pp neutrinos, their arrival in the active phase of the solar cycle, or coronal mass ejections will be much more. In this case, the radiation of excited atoms of nitrogen and oxygen will be observed as the aurora. Due to the fact that in areas of the magnetic poles the synthesis of NE is very slowed down, the auroral zone usually have the form of rings. At the same time, a stable orientation of the magnetic axes of NN along magnetic field lines directly above the magnetic pole, conversely promotes condensation of NN into MN. Apparently this is what causes the phenomenon of auroral kilometric radiation (AKR). The trigger that starts AKR, is the cyclotron radio emission of electrons moving toward the poles in a spiral along the magnetic field lines. As a result, amplification by reactions of condensation of MN leads to powerful radio emission. As we found out above, the molecular aggregations of neutrinium have a structure that suggests layered stacks of NN in MN. It is logical to assume that the magnetic axis of NN will be directed perpendicular to the layers of NN in MN. Since photons are generated in the location of the kappa-bonds between NN, it determines the transverse direction of radiation with respect to the magnetic axes of NN. That is why AKR propagates predominantly perpendicular to the magnetic axis of the Earth.

6. Herbig-Haro objects

All young stars at the beginning of its life cycle are characterized by a narrow directed polar gas ejections. During the initial gravitational contraction of the proto-star in its vicinity is created increased concentration of galactic antineutrinium. Once in the nucleus of young stars are starting to go thermonuclear reactions then neutrinium synthesized and ejected by star takes the annihilation with the galactic antineutrinium. In the field of magnetic poles NN tend to condense among themselves. Condensation of stellar and galactic NN is accompanied by annihilation, more intense in the polar regions. Orientation of NN along the magnetic lines promotes the release of LM along the magnetic axis of the star. Throughout ejections, there continues to go NE synthesis restoring the equilibrium mass number NE, and X-rays accompanying synthesis, stimulates the gas atoms of the proto-stellar nebulae. As a result, the gas emits in the visible and infrared range. At the same time in the polar ejection condensation of MN occurs, accompanied by radio emission. Over tens and hundreds of years, the flow of stellar neutrinium largely dissipates galactic LM, annihilate with it in the vicinity of the star, and eventually the radiation of polar ejection fades.

7. Radio pulsars

It is considered that the radio emission of pulsars is generated by charged particles that escape from the magnetic poles of the rotating neutron star (NS). It is assumed that the magnetic axis does not coincide with the axis of rotation. We consider a model in which the radio emission is generated at the magnetic poles together as by charged particles and by neutral nuclei of antinyutrinium. Immediately after its formation each NS starts accumulating galactic antineutrinium. Within a few decades, the density of LM on the surface of new NS becomes many orders of magnitude higher than in the interstellar medium. When accretion and scattering of LM beginning balance each other, the density distribution of LM takes the form:

$$\rho_{DM}(r) = k_D\ \rho_A\ (r_{NS}\,/\,r)^{2.5}\ , \qquad (8)$$

where ρ_A is limiting density of LM ($\rho_A = 2.72\times10^{14}$ kg/m^3), r_{NS} is estimated ("neutron") radius of NS ($r_{NS} = 11200$ м), k_D — density factor ($k_D = 1.41\times10^{-14}$) Density factor k_D is chosen so that the density of LM on the sphere of beginning of accretion (SBA) coincided with the average density of the interstellar medium of LM. On the galactic radius of the solar system the radius of SBA is arbitrarily taken equal to 1.2 radius of Neptune's orbit, and the average density of LM is taken equal to 7.58×10^{-22} kg/m^3 (0.425 GeV/s^2/cm^3). Thus we find that the average density of LM at the surface of NS is 3.84 kg/m^3, or 2.15×10^{23} NN in 1 cm^3 (if we assume that the galactic nucleus of antineutrinium have an average mass number 20 and mass 10 MeV). Average distance traveled by NN with such density of LM before the collision with each other will be comparable with the average distance traveled by air molecules, but with the concentration of molecules 10^5 times less (as many times the size of atoms larger than the atomic nuclei and the nuclei of LM). By comparison, in the terrestrial atmosphere the same concentration of air molecules takes place at an altitude of about 16 km. The electric current in iron crust, which induces the magnetic field, compresses star resulting NS takes triaxial ellipsoid shape. Rotating elongated NS intensively stirred and heated LM from the surface to turbopause, which will be located at a radius of about 1400 km. The wind speed of LM at the surface of NS is of the order of hundreds or thousands of m/s. Strict orientation of the magnetic axes of NN along the magnetic axis of NS above the magnetic poles causes an exceptional propensity of NN to condensation into MN. At the exit of polar regions MN splits completely to the original NN. Like AKR, the radio emission of pulsars (REP) is distributed in two parallel planes passing over the magnetic poles, exactly perpendicular to the magnetic axis of NS. At that moment, when the pair of planes of radio emission coincides with the line of sight, is registered radio pulse. As well as the AKR, REP is stimulated emission, and the trigger is the synchrotron radio emission of electrons (SREE) that penetrate into the NS over the magnetic poles. Because LM is heated near NS, REP receives a significant Doppler broadening, up to several thousand times. That is why the spectrum of REP is in a narrow range at the high end of the Doppler broadening. Since one of the areas of radiation moves away from us, and the other moves on us, then the spectrum of the radio pulse has a characteristic form with two peaks, with a maximum at a frequency ν_m and a kink at a higher frequency ν_c. It would seem that the maximum of spectral density shall be in the high kink corresponding to radiation from oncoming region. However, we need to take into account the magnetic hysteresis of LM, which consists in the delayed rotation of the magnetic axes of NN following the change in the magnetic field of NS. Due to the hysteresis region of stimulated emission from the condensation of NN into MN in front of a narrow cone of SREE will be much thinner than the rear volume of NN potentially ready to condensation into MN. That is why the radio flux in the rear direction is stronger than in the front. From the redshift of frequency ν_m, and the blue shift of frequency ν_c, we can determine the linear velocity of LM in place of radiation and figure out to what degree the movement of LM is related to the rotation of NS.

8. The spiral arms of galaxies

There are several models of the spiral structure of galaxies, of which the most accepted is the one that explains the spiral arms by proliferation of density waves. Some models are based on the effects of gravitational perturbations from conglomerates of DM flocking to the galaxy from the surrounding space. But have we ever thought when looking at images of spiral galaxies, that they are similar on a rotating fireworks? As we found out earlier [3], in the galactic bulge occurs increased intensity of annihilation of neutrinium stellar LM (SLM) and antineutrinium galactic native LM (NLM). Suppose that in the bulge of spiral galaxies the magnetic field acquire configuration of double dipole so that the axis of the galactic magnetic dipoles (GMD) are aligned and lie in the plane of the galactic disk. At the magnetic poles of GMD are created favorable conditions for the condensation of NN, and this means that there is significantly increases the intensity of the annihilation of SLM and NLM. On the external magnetic poles annihilation of LM is accompanied by expiration outward of collimated streams consisting of partially annihilated nuclei of NLM and SLM. Continuous supply of SLM from stars provides long-term nature of annihilation and ejections of LM, and the rotation of galaxies causes twisting of streams into the spiral arms. When the main GMD facing each other oppositely charged poles then arises between them a galactic bar, if the internal poles have the same charge, then the bar will not occur. In addition to the two main GMD in the bulge of spiral galaxies can occur secondary GMD manifested less pronounced and interrupted spiral fragments. If GMD appears in the center of galaxies (spiral or elliptical), it will have an orientation that coincides with the axis of rotation of the galactic nucleus. Such GMD generate bipolar gamma-ray bubbles and relativistic jets.

9. Quasars and active galactic nuclei

It is considered that the emission of quasars formed as a result of accretion of gas-dust matter (GDM) to the central supermassive black hole. In our model, the concept of "black hole" is absent [1], and as a central object acts a supermassive neutron collapsar (SMNC), surrounded by a halo of LM. As an energy source of quasars we will consider not the energy of accretion of GPM, but the energy of annihilation of admixture of anti-LM (AALM) with NLM. In the role of NLM can act as antineutrium and neutrinium, depending on whether a given quasar is a part of the galactic walls or filaments composed of matter or antimatter. This means, and taken as a postulate that the universe consists of equal amounts of matter and antimatter, divided among themselves on the level of galactic filaments and walls. Imagine a large-scale structure of the universe in the form of close packing of truncated octahedra-voids, adjacent faces of which coincide. Galactic walls lie on the faces of the truncated octahedra-voids, and on the edges lie galactic filaments. In each edge-filament intersect three imaginary faces, but actually only two walls (only of matter or only of antimatter) and the third wall (of antimatter or matter) is separated from the filament by slit whose width is comparable to the thickness of walls. In some places slit is not enough empty or too narrow. In these places to NLM mixed anti-LM. Where LM is in a rarefaction, the annihilation between NLM and AALM will be too weak to show themselves, at least locally. However, near the central SMNC where the density of LM increases significantly, the annihilation of AALM and NLM becomes more intense. Since the accretion of LM onto central SMNC lasts continuously for billions of years, then in the early epoch in a sufficiently dense layer of halo there is an area of high-intensity annihilation where AALM completely burn. Assuming that some part (up to 5%) of AALM annihilates in higher and more rarefied layers, we assume that the bulk of the AALM completely annihilates in a layer of halo with density of LM equivalent by the mean free path to air molecules of that part of the earth's atmosphere, which lies between the mesopause (height of 80 km) and stratopause (height of 50 km). Let us take as a model of a quasar the mass model of the object Sagittarius A*, based on modeling of the orbital motion of the star S0-2. The density distribution of LM near central SMNC can be written as:

$$\rho_{DM}(r) = k_D \, \rho_A \, (r_{CC} / r)^{2.5} \, , \qquad (9)$$

where r_{CC} is radius of the central SMNC ($r_{CC} = 3.5\times10^5$ m), k_D is density factor ($k_D = 0.97$).

For quasar comparable by mass to Sgr A*, a layer of halo, where annihilates 95% of AALM, will be located in a radius of 4.5 to 26 AU (i.e. would fit between the orbits of Jupiter and Neptune). Mass of LM in this area will be about 280 thousand of $M_\odot$, which is about 6 times the mass of the central SMNC. LM accretion rate at the outer radius of annihilation area will be about 0,1 $M_\odot$ per second. Let us take the nearest quasar 3C 273, which luminosity is greater than that of the sun about 1 trillion times. If we accept its accretion rate the same as at Sgr A*, the quasar 3C 273 must spend every second about 0.33% of accreting LM. In this case, the concentration of AALM in NLM in the host galaxy of 3C 273 will be 0.1-0.2%. But if we claim that the quasar radiation is caused by annihilation of LM, it will be logical to assume that the emission of AGN also be due to the annihilation of AALM and NLM. Continuing, we can assume that the admixture of anti-LM in NLM in a low background concentration is present everywhere in the universe. Then in the universe must constantly go background annihilation of AALM and NLM. As manifestations of such a background annihilation, we can consider the reionization of the intergalactic gas and extragalactic background light.

10. Extragalactic background light

As is known, EBL is in the range from the ultraviolet to the infrared and is the second most powerful source of diffuse background radiation of the universe after the CMB. Our model assumes a three-component composition of EBL. As the first component is the relic radiation from the burst of synthesis of NE in the epoch of recombination. As the second component is the diffuse radiation from a continuously running background annihilation of AALM and NLM. As the third component is the radiation of background NE synthesis, which involves NN after partial annihilation of LM

Table 2: Components of the extragalactic background light

The primary source of radiation	The photon energy (wavelength) at the moment of radiation	The era of radiation	Wavelength currently
Relic burst of NE synthesis	2 – 6 keV	$z \approx 1089$	230 – 670 nm
Background annihilation of LM	0.25 meV – 0.62 MeV (5×10^{-3} – 2×10^{-12} m)	$1089 > z > 0$	5.4 – 2×10^{-12} m
Background synthesis of NE	3.5 keV	$1089 > z > 0$	3.8×10^{-7} – 3.5×10^{-10} m

In the bulges of galaxies and in galactic superclusters increased concentration of SLM leads to the increased annihilation of LM and reductions of the average mass number of NE. This entails increasing the intensity of the background NE synthesis, restores the equilibrium mass number of NE. Thus, the recently discovered X-ray line with an energy of 3.5 keV observed in large galaxies is due to the increased intensity of the synthesis of NE.

11. Conclusions

Based on the similarity of the properties of neutrinos and DM particles, we have built a new model of LM, in which neutrinos are endowed with the ability to form Cooper pairs and merge into the nuclei of deutrinium, the lightest element of LM. Making a list of NE and studying their structure, we found that the neutrinos in NN can be joined together by two types of bonds, alpha and kappa. Chemistry of NE describes reactions in which fusion of CNP occurs and is changed the mass number and the aggregate state of NE. CNE has allowed us to explain a number of astrophysical phenomena in which LM closely interact with ordinary matter. Learning to detect and measure LM, we can produce LM. And then we become participants of the cosmic performance of civilizations.

References

[1] D. Skripachov, A new model of gravitation. viXra:1404.0463, (2014)
[2] D. Skripachov, Virtual crossword of Grand unification. viXra:1405.0305, (2014)
[3] D. Skripachov, Two-level mass model of the Milky Way. viXra:1408.0106, (2014)
[4] G. Angloher, et al., Results from 730 kg days of the CRESST-II Dark Matter Search. Eur. Phys. J. C **72** 1971, (2012), arXiv:1109.0702, (2011)
[5] R. Bernabei, et al., Final model independent result of DAMA/LIBRA-phase1. 16th Lomonosov Conference, Moscow, (August 2013), arXiv:1308.5109, (2013)
[6] S. Chang, J. Liu, A. Pierce, N. Weiner, I. Yavin, CoGeNT Interpretations. JCAP 08, 018, (2010), MCTP-10-16, arXiv:1004.0697, (2010)
[7] C. E. Aalseth, P.S. Barbeau, J. Colaresi, et al., Search for An Annual Modulation in Three Years of CoGeNT Dark Matter Detector Data, arXiv:1401.3295, (2014)
[8] E. Armengaud, et al., (EDELWEISS Collaboration), A search for low-mass WIMPs with EDELWEISS-II heat-and-ionization detectors. Phys. Rev. D **86** 051701, (2012), arXiv:1207.1815, (2012)
[9] E. Aprile, et al., (XENON100 Collaboration), Response of the XENON100 Dark Matter Detector to Nuclear Recoils. Phys. Rev. D **88** 012006, (2013), arxiv:1304.1427, (2013)
[10] R. Agnese, et al., CDMSlite: A Search for Low-Mass WIMPs using Voltage-Assisted Calorimetric Ionization Detection in the SuperCDMS Experiment. arXiv:1309.3259, (2013)
[11] C. Boehm, P. Fayet, J. Silk, Light and Heavy Dark Matter Particles. Phys. Rev. D **69** 101302, (2004), arXiv:hep-ph/0311143, (2003)
[12] M. Loewenstein, A. Kusenko, Dark Matter Search Using Chandra Observations of Willman 1, and a Spectral Feature Consistent with a Decay Line of a 5 keV Sterile Neutrino. APJ **714** 652, (2010), arXiv:0912.055, (2009)
[13] E. Bulbul, M. Markevitch, A. Foster, R. K. Smith, M. Loewenstein, S. W. Randall, Detection of An Unidentified Emission Line in the Stacked X-ray spectrum of Galaxy Clusters. arXiv:1402.2301, (2014)
[14] A. Boyarsky, O. Ruchayskiy, D. Iakubovskyi, J. Franse, An unidentified line in X-ray spectra of the Andromeda galaxy and Perseus galaxy cluster. arXiv:1402.4119, (2014)
[15] J. F. Beacom, N. F. Bell, S. Dodelson, Neutrinoless Universe. Phys. Rev. Lett. **93** 121302, (2004), arXiv:astro-ph/0404585, (2004)
[16] R. Jr. Davis, D. S. Harmer, Solar Neutrinos. Brookhaven National Laboratory, Upton, New York, (1965)
[17] J. N. Bahcall, M. H. Pinsonneault, S. Basu, Solar Models: current epoch and time dependences, neutrinos, and helioseismological properties. ApJ **555** 990, (2001), arXiv:astro-ph/0010346, (2001)
[18] J. N. Abdurashitov, et al., (SAGE Collaboration), Measurement of the solar neutrino capture rate with gallium metal. III: Results for the 2002--2007 data-taking period. Phys. Rev. C **80** 015807, (2009), arXiv:0901.2200, (2009)
[19] K. Eguchi, et al., (KamLAND Collaboration), First Results from KamLAND: Evidence for Reactor Anti-Neutrino Disappearance. Phys. Rev. Lett. **90** 021802, (2003), arXiv:hep-ex/0212021, (2002)
[20] G. Bellini, et al., (Borexino Collaboration), Precision measurement of the ^{7}Be solar neutrino interaction rate in Borexino. Phys. Rev. Lett. **107** 141302, (2011), arXiv:1104.1816, (2011)
[21] G. Bellini, et al., (Borexino Collaboration), First evidence of pep solar neutrinos by direct detection in Borexino. Phys. Rev. Lett. **108** 051302, (2012), arXiv:1110.3230, (2011)
[22] A. Gando, et al., (KamLAND Collaboration), ^{7}Be Solar Neutrino Measurement with KamLAND. arXiv:1405.6190, (2014)
[23] V. Antonelli, L. Miramontia, C. Peña-Garay, and A. Serenelli, Solar Neutrinos. Advances in High Energy Physics, vol. 2013, (2013), arXiv:1208.1356, (2012)
[24] M. M. Nieto, A. C. Hayes, C. M. Teeter, W. B. Wilson, W. D. Stanbro, Detection of Antineutrinos for Non-Proliferation. Nucl. Sci. Engin. **149** 270, (2005), arXiv:nucl-th/0309018,

(2004)
[25] F. P. An, et al., (Daya Bay Collaboration), Improved Measurement of Electron Antineutrino Disappearance at Daya Bay. Chinese Phys. C **37** 011001, (2013), arXiv:1210.6327, (2012)
[26] P. D. Ewing, S. W. Kercel, K. Korsah, R. T. Wood, Electromagnetic Compatibility in Nuclear Power Plants. Global '99: International Conference on Future Nuclear Systems, Jackson Hole, WY, (1999)
[27] L. Wolfenstein, Neutrino oscillations in matter. Phys. Rev. D **17** 2369, (1978)
[28] A. Yu. Smirnov, The MSW effect and Solar Neutrinos, 10th workshop on Neutrino Telescopes, Venice, (March 2003), arXiv:hep-ph/0305106, (2003)
[29] H. E. George, F. Ellerman, S. B. Nicholson, A. H. Joy, The Magnetic Polarity of Sun-Spots. APJ **49** 153, (1919)
[30] E. Tandberg-Hanssen, A. G. Emslie, The physics of solar flares. Cambridge University Press, Cambridge, (1988)
[31] R. A. Howard, A Historical Perspective on Coronal Mass Ejections. Geophysical Monograph Series **165** 7, (2006)
[32] A. O. Benz, Radio emission of the quiet Sun. Trümper, J.E. (ed.). SpringerMaterials - The Landolt-Börnstein Database. Springer-Verlag Berlin Heidelberg, (2009).
[33] Zhu L., R.W. Schunk, and J.J. Sojka, Polar cap arcs: A review, Journal of Atmospheric and Terrestrial Physics **59** 1087, (1997)
[34] A. Bhardwaj, X-Ray Emission from Jupiter, Saturn, and Earth: A Short Review. Advances in Geosciences **3** 215, (2006), arXiv:astro-ph/0605282, (2006)
[35] J. Hanasz, H. de Feraudy, R. Schreiber, and M. Panchenko, Pulsations of the auroral kilometric radiation. Journal of Geophysical Research: Space Physics **111** A3, (2006)
[36] R. A. Treumann, W. Baumjohann, R. Pottelette. Electron-cyclotron maser radiation from electron holes: Downward current region. Ann.Geophys. **30** 119, (2012), arXiv:1110.4286, (2011)
[37] J. Lopez-Santiago, C. S. Peri, R. Bonito, M. Miceli, J. F. Albacete-Colombo, P. Benaglia, E. de Castro, Evidence of non-thermal X-ray emission from HH 80. ApJ 776 L22, (2013), arXiv:1309.4256, (2013)
[38] L. F. Rodriguez, B. Reipurth, H.-F. Chiang, Radio Continuum Sources associated with the HH~92 and HH~34 Jets. arXiv:1405.6638, (2014)
[39] R. N. Manchester, J. H. Taylor, Pulsars. W. H. Freeman, San Francisco, (1977)
[40] A. A. Deshpande, J. M. Rankin, Pulsar Magnetospheric Emission Mapping: Images and Implications of Polar-Cap Weather. ApJ **524** 1008, (1999), arXiv:astro-ph/9909398, (1999)
[41] A. Valinia, F. E. Marshall, RXTE Measurement of the Diffuse X-ray Emission From the Galactic Ridge: Implications for the Energetics of the Interstellar Medium. ApJ **505** 134, (1998), arXiv:astro-ph/9804012, (1998)
[42] R. Krivonos, M. Revnivtsev, E. Churazov, et al., Hard X-ray emission from the Galactic ridge. A&A **463** 957, (2007), arXiv:astro-ph/0605420, (2006)
[43] J. F. Navarro, C. S. Frenk, S. D. M. White, The Structure of Cold Dark Matter Halos. ApJ **462** 563, (1996), arXiv:astro-ph/9508025, (1995)
[44] D. Minniti and M. Zoccali, The Galactic bulge: a review. Proceedings of IAU **3** 323, (2007), arXiv:0710.3104, (2007)
[45] M. Haverkorn, V. Heesen, Magnetic fields in galactic haloes. Space Science Reviews **166** 133, (2012), arXiv:1102.3701, (2011)
[46] R. Beck, R. Wielebinski, Magnetic fields in galaxies. Planets, Stars and Stellar Systems, **5** 641, (2013), arXiv:1302.5663, (2013)
[47] Meng Su, T. R. Slatyer, D. P. Finkbeiner, Giant Gamma-ray Bubbles from Fermi-LAT: AGN Activity or Bipolar Galactic Wind? APJ **724** 1044, (2010), arXiv:1005.5480, (2010)
[48] E. Carretti, R. M. Crocker, L. Staveley-Smith, et al., Giant Magnetized Outflows from the Centre of the Milky Way. Nature **493** 66, (2013), arXiv:1301.0512, (2013)
[49] D. Hooper, T. R. Slatyer, Two emission mechanisms in the Fermi Bubbles: A possible signal of annihilating dark matter. Physics of the Dark Universe **2** 118, (2013), arXiv:1302.6589, (2013)
[50] Z. Berezhiani, A. D. Dolgov, I. I. Tkachev, Dark matter and generation of galactic mag-

netic fields. EPJC **73** 2620, (2013) , arXiv:1307.6953, (2013)
[51] N. Prantzos, On the 511 keV emission line of positron annihilation in the Milky Way. New Astronomy Reviews 52 457, (2008), arXiv:0809.2491, (2008)
[52] E. D'Onghia, M. Vogelsberger, L. Hernquist, Self-Perpetuating Spiral Arms in Disk Galaxies. ApJ **766** 34, (2013), arXiv:1204.0513, (2013)
[53] D. L. Meier, The Theory and simulation of relativistic jet formation: Towards a unified model for micro- and macroquasars. New Astron. Rev. **47**, (2003), arXiv:astro-ph/0312048, (2003)
[54] B. V. Komberg, A. V. Kravtsov, V. N. Lukash, The search and investigation of the Large Groups of Quasars. MNRAS **282** 713, (1996) , arXiv:astro-ph/9602090, (1996)
[55] A. G. Cohen, A. De Rújula, and S. L. Glashow, A Matter-Antimatter Universe? ApJ **495** 539, (1998), arXiv:astro-ph/9707087, (1997)
[56] Y. Shen , M. A. Strauss, N. P. Ross, et al., Quasar Clustering from SDSS DR5: Dependences on Physical Properties. ApJ **697** 1656, (2009), arXiv:0810.4144, (2008)
[57] T. J.-L. Courvoisier, The Bright Quasar 3C 273. A&A Rev. **9** 1-32, (1998), arXiv:astro-ph/9808147, (1998)
[58] L. Meyer, A. M. Ghez, R. Schödel, et al., The Shortest Known Period Star Orbiting our Galaxy's Supermassive Black Hole. Science **338** 84, (2012), arXiv:1210.1294, (2012)
[59] Space environment (natural and artificial) -- Earth upper atmosphere. ISO/FDIS 14222, www.iso.org, (retrieved in July 2013)
[60] N. Jarosik, C. L. Bennett, J. Dunkley, et al., Seven-Year Wilkinson Microwave Anisotropy Probe (WMAP) Observations: Sky Maps, Systematic Errors, and Basic Results. ApJS **192** 14, (2011), arXiv:1001.4744, (2010)
[61] M. G. Hauser, The Far Infrared and Submillimeter Diffuse Extragalactic Background. ASP Conf. Ser. **204** 101, (2001), arXiv:astro-ph/0105550, (2001)
[62] K. Mattila, K. Lehtinen, P. Vaisanen, G. von Appen-Schnur, C. Leinert, Spectrophotometric measurement of the Extragalacic Background Light . IAU Symposium **284**, arXiv:1111.6747, (2001)